Enhanced Phosphorescence Emission by Incorporating Aromatic Halides into an Entangled Coordination Framework Based on Naphthalenediimide

Virginia Martínez-Martínez, Rebeca Sola-Llano, Shuhei Furukawa, Yohei Takashima, Iñigo López Arbeloa, and Susumu Kitagawa

https://doi.org/10.1002/cphc.201402188

ChemPhysChem 2014,15, 2517 – 2521

Enhanced Phosphorescence Emission by Incorporating Aromatic Halides into an Entangled Coordination Framework Based on Naphthalenediimide

Virginia Martínez-Martínez,*[a] Rebeca Sola Llano,[a] Shuhei Furukawa,[b] Yohei Takashima,[b] Iñigo López Arbeloa,[a] and Susumu Kitagawa[b]

Phosphorescence emission at room temperature is turned on in an entangled porous coordination polymer (PCP) with naphthalenediimide (NDI) as chromophore, by incorporating halogenated guests into the pores. The phosphorescent efficiency is drastically increased by the incorporation of aromatic halide guests in comparison with the incorporation of nonaromatic derivatives. Aromatic halide guests trigger a structural transformation, which allows a strong interaction with the NDI ligand in the framework through charge-transfer complexation, and provides an extra population process of the triplet state. The long-lived photoinduced triplet states, with an emission wavelength in the red region of the visible spectrum, demonstrated by this PCP, may open the door for potential uses, for example, as singlet-oxygen generators or for bio-imaging applications.

1. Introduction

Many transition-metal complexes, such as Os, Ru, Pd, Pt, Ir, or Au complexes, exhibit room-temperature phosphorescence (RTP), as a result of the promotion of intersystem crossing (ISC) in organic ligands through the triplet metal-to-ligand charge-transfer state.[1–5] However, RTP from pure organic chromophores is generally inefficient, because a transition between states with different multiplicity (T_1–S_0) is forbidden and they also suffer many nonradiative deactivation pathways, which are mainly caused by intramolecular motions (molecular rotation and vibration) or intermolecular interactions (solute–solvent and solute–solute collisions or quenching by molecular oxygen).[5–7] One way to induce RTP in organic compounds is to restrict molecular motions by increasing the rigidity of the chromophore, for instance, by crystallizing them in the solid state or by physically confining them into a restricted space by using host matrices, such as cyclodextrins, micelles, or cucurbiturils.[8–12] Another alternative is to increase the population of the triplet state by using spin-forbidden transition enhancers.[13–16] In this regard, the phosphorescence quantum yield of chromophores can be increased by adding halogen substituents to the molecular skeleton (internal heavy-atom effect) or by the presence of halide atoms located very close to the phosphor (external heavy-atom effect). In the latter case, a very high local concentration of heavy atoms in solution is required to efficiently increase the ISC to the triplet state.

[a] Dr. V. Martínez-Martínez, R. Sola Llano, Prof. I. López Arbeloa
Dpto. Química Física, Universidad del País Vasco (UPV/EHU)
Aptdo. 644, 48080 Bilbao (Spain)
E-mail: virginia.martinez@ehu.es

[b] Dr. S. Furukawa, Dr. Y. Takashima, Prof. S. Kitagawa
Institute for Integrated Cell-Material Sciences (WPI-iCeMS)
Kyoto University, Yoshida, Sakyo-ku, Kyoto 606-8501 (Japan)

One strategy to generate RTP in organic molecules is to arrange them regularly so that they are a short distance from heavy atoms. We propose the use of porous coordination polymers (PCPs) or metal–organic frameworks (MOFs), because of their unique porous properties, which are easily tuned, and their crystalline nature. By embedding an organic phosphor into a framework scaffold as a building block and accommodating halide derivatives as guests into the nanopores, all of the above requirements can be fulfilled; the ordered sequence of molecular phosphors avoids self-quenching, restricts their molecular motions, and allows strong interactions with the halides incorporated into the pores.

Here, we chose the entangled PCP $[Zn_2(bdc)_2(dpNDI)]_n$ (bdc = 1,4-benzenedicarboxylate, dpNDI = *N*,*N*′-di(4-pyridyl)-1,4,5,8-naphthalenediimide), because naphthalenediimide (NDI) itself is an appropriate candidate for phosphoresence emission, as its very short fluorescence lifetime (few ps) originates from the rapid ISC from the excited π–π^* singlet state to the close lying n–π^* triplet state.[17] Phosphorescence emission has previously been observed for similar NDI derivatives mixed with iodoethane when frozen at 77 K.[18] More importantly, RTP has already been recorded from dpNDI as part of the above PCP with iodobenzene as the guest molecule;[19] this is a consequence of the induced-fit structural transformation (See the Supporting Information, Figure S1) already demonstrated in this PCP after the inclusion of different R–phenyl guests, which has shown an interesting guest-dependent luminescent response. The so-called dynamic confinement is triggered by the strong interaction between the dpNDI moiety and the aromatic guests that enhances the charge-transfer (CT) complexation between them.[19,20] Herein, we study the photophysical aspects of phosphorescence of the entangled PCP $[Zn_2(bdc)_2(dpNDI)]_n$ by monitoring the temperature-dependent emission spectra and their respective decay curves, when different aro-

matic and nonaromatic halide derivatives are accommodated in the modal pores of its framework.

2. Results and Discussion

First, this entangled PCP undergoes a structural transformation after the inclusion of different phenyl halide guests (X–phenyl: X = Cl, Br, or I) into the PCP, as evidenced by the powder X-ray diffraction (PXRD) patterns (Figure S2). This structural change was expected, because the ionization potentials (IP; Table 1) of the guests were lower than the IP of benzene, which suggests the significance of CT complexation between the electron donor of guests and the electron acceptor of dpNDI; a molecule with a higher ionization potential, such as benzonitrile (IP = 9.70 eV), is not sufficiently electron-donating to permit CT complexation and therefore does not generate the inherent induce-fit structural transformation mechanism (Figure S2).

Table 1. Ionization potential (IP), fluorescence emission maxima (λ_{fl}), mean fluorescence lifetime ($<\tau>_{fl}$), phosphorescence emission maxima (λ_{ph}) and emission quantum yield (φ) of different guests.

Guest[a]	IP [eV]	λ_{fl} [nm]	$<\tau>_{fl}$ [ns]	λ_{ph} [nm]	Φ[a] [%]
benzonitrile	9.70	421	–	–	<1
benzene	9.25	439	5.0	–	5
Toluene[17,18]	8.82	476	14.8	–	22
Cl-benzene	8.35	452	2.5	–	~1
Br-benzene	8.98	455	2.4	628	~1
I-benzene	8.73	–	–	637	3
I-ethane	9.33	–	–	619	<1

[a] Quantum yield recorded in the whole visible range (400–750 nm).

In comparison with the inclusion of nonhalogenated aromatic guests, a marked quenching of the fluorescence emission ($\varphi_{fl} \leq 0.01$), together with a sharp decrease in fluorescence lifetimes, is obtained with aryl halide guests (Table 1).[19,20] The PCP shows an interesting switch from fluorescence to phosphorescence emission at room temperature as the size of the halogen atom increases (X = Cl < Br < I; Table 1). Thus, the fluorescence band attributed to the NDI–guest CT complexes[19,20] decreases as a new red-shifted phosphorescence band at around 630 nm appears. The assignment of the red band to phosphorescence emission is supported by the acquisition of the spectra after a delay of 50 μs after the excitation flash to remove any fluorescence interference (Figure 1).

To study the effect of CT complexation between halogenated aromatic guests (donor: D) and NDI (acceptor: A) on the phosphorescence process, the nonaromatic guest iodoethane was also incorporated into the pores as a reference. Thermogravimetric analysis (TGA) shows that two molecules are incorporated in the pores for both guests, iodobenzene and iodoethane (Figure S3).

Although the phosphorescence emission of the PCP incorporating iodoethane was detected at room temperature, its intensity was around six times weaker than that registered for the homologous aromatic guest, iodobenzene, at both 298 and 77 K (Figure 2). Furthermore, the phosphorescence emission intensity registered for bromobenzene, which contains a lighter halogen atom, is twice or three times higher than that obtained for iodoethane at 298 and 77 K, respectively. Notably, the emission spectra recorded for the pure ligand dpNDI in iodoethane and iodobenzene as solvents do not show any emission band at room temperature and only a reminiscent phosphorescent band placed at around 615 nm has been registered at 78 K in both solvents (Figure S4).

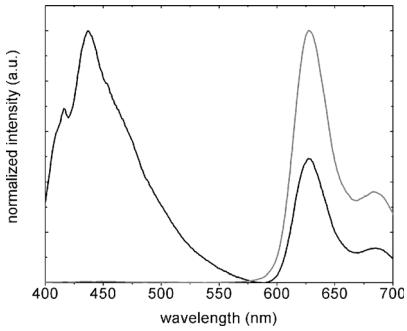

Figure 1. Height-normalized emission spectra of PCP with bromobenzene as guest. Black curve: steady-state excitation. Grey curve: microsecond pulse lamp excitation and signal recorded at 50 microseconds after pulse.

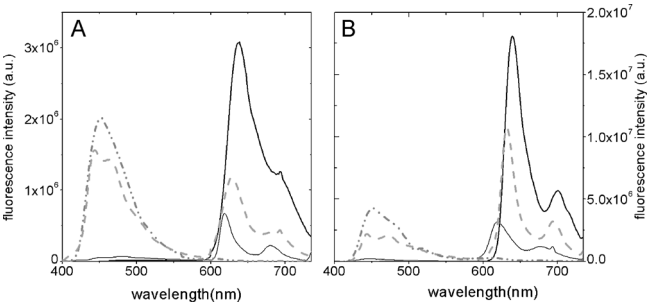

Figure 2. Steady-state emission spectra for different halogenated guests: iodobenzene (——), iodoethane (——), bromobenzene (– – –), and chlorobenzene (–•–•–) at 298 (A) and 77 K (B).

These observations indicate several characteristics offered by the PCP. 1) On the one hand, the similarity of the phosphorescence bands registered in this PCP to those obtained for dpNDI ligand (Figure S4) and other similar NDI derivatives in iodide solvents when frozen at 77 K,[17,18,21,22] indicates that the final triplet state lies on the dpNDI ligand and the emission is not altered by metal–ligand interactions. On the other hand, the possibility of detecting phosphorescence emission at room temperature in most of the samples (except for chlorobenzene) is related to the crystalline nature of PCP, which contributes to reduce triplet nonradiative deactivation pathways by avoiding self-quenching of the dpNDI phosphor and other intermolecular interactions typically observed in the liquid phase. 2) The physical confinement of the halide guests in the pores favors a higher spin-orbit interaction compared with the solution.[22] 3) The higher phosphorescence efficiency obtained for aromatic halide guest, with respect to the nonaromatic analogue, indicates a more effective population of the triplet state as a result of the enhanced dpNDI–halide interactions and, consequently, a more effective spin-orbit coupling.

CT complexation between the aryl halide guest and dpNDI can also contribute to the enhancement of the phosphorescence emission through extra population processes of the triplet state, as illustrated in Scheme 1. The excitation spectrum of

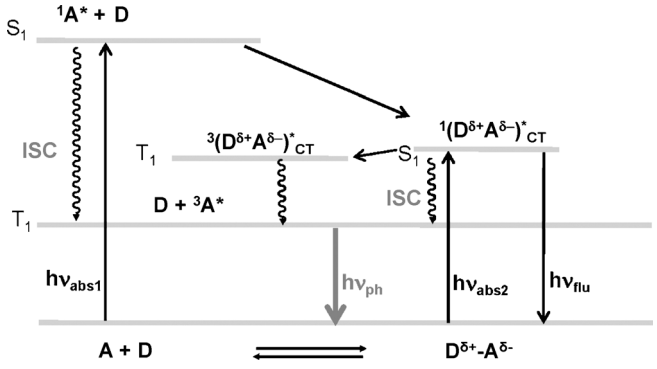

Scheme 1. Energy-level diagram of the emissive species and processes in the PCP. The triplet state can be populated by either ISC from dpNDI or from the CT excited states. A = dpNDI, abs = absorption, D = phenyl halide guest, flu = fluorescence, ph = phosphorescence, S = singlet State, T = triplet State.

the PCP with iodobenzene obtained at its phosphorescence emission maximum (635 nm) shows a prominent shoulder in the lower energy region (at 430–470 nm) with respect to the main absorption band of dpNDI (λ_{ab} ~ 380 nm; Figure S5), thus indicating the contribution of the CT excited state in the population of the final phosphorescence low-lying triplet-excited state of dpNDI. In fact, similar mechanisms have been described in previous phosphorescence studies of similar NDI chomophores as electron acceptor moieties in donor–acceptor (D–A) covalent dyads at 77 K.[21,22]

Decay curves were obtained at different temperatures (Table 2) to gain further information on the phosphorescence process. The mean lifetimes obtained are in the typical time range for phosphorescence emission of organic phosphors.[23] The mean lifetimes for the triplet excited state of the PCPs incorporating iodobenzene and iodoethane are similar to each other (around several tens/hundreds microseconds), whereas PCPs incorporating brominated or chlorinated guests show much longer mean lifetimes (several milliseconds). According to the equation $\tau_{ph} = 1/(k_{ph}+k_{nr})$, this difference could be assigned to a reduction in the phosphorescence radiative constant k_{ph}, because of the lower spin-orbit coupling induced by the Br or Cl atoms, which are lighter than the I atom.

The phosphorescence emissions and their corresponding lifetimes gradually increase as the temperature decreases (Figure 3); this trend is attributed to the reduction of nonradiative routes (k_{nr}), that is, reduction of internal conversion process and bimolecular collision under freezing conditions, particularly when the temperature is cooled to below the melting point of each guest.

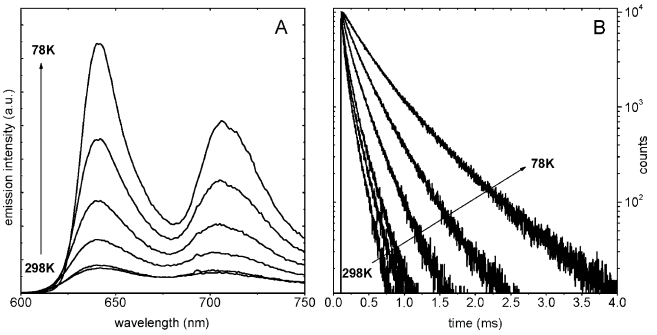

Figure 3. A) Steady-state emission spectra and B) phosphorescence decay curves for iodobenzene at different temperatures (298, 278, 228, 178, 128, and 78 K).

Finally, all samples show biexponential kinetics (Figure S6). The reason for this behavior is not clear and could be attributed to several causes: 1) the existence of different phosphorescence species (i.e. ^{3}dpNDI and ^{3}CT), 2) two different mechanisms of populating the triplet state (i.e. directly by dpNDI and from the CT complex states), or 3) different spin-orbit coupling efficiencies (i.e. halide atoms at different distances from dpNDI). Taking into account the first two possibilities, the complexation between the dpNDI and the aromatic guests must be involved (Scheme 1). However, option 3 could be considered as the most important cause, because a biexponential fit is also registered for the nonaromatic guest. Indeed, it has been already reported that two geometrically different adsorption sites in this PCP[20] provide different positions for guests with respect to the dpNDI phosphor (Figure S7).

Table 2. Phosphorescence lifetimes of iodobenzene, iodoethane, bromobenzene, and chlorobenzene at different temperatures (τ_i), statistical weight (A_i), and average phosphorescence lifetime ($<\tau>$).[a]

T [K]	Iodothane $\tau_1(A_1)\ \tau_2(A_2)\ <\tau>$ [us]	Iodobenzene $\tau_1(A_1)\ \tau_2(A_2)\ <\tau>$ [us]	Bromobenzene $\tau_1(A_1)\ \tau_2(A_2)\ <\tau>$ [ms]	Chlorobenzene[b] $<\tau>$ [ms]
78	230 (59) 550 (41) 430	275(66) 620(33) 458	4.3(48) 7.9(52) 6.7	≈9
128	140(66) 360(33) 264	151(56) 347(44) 277	2.3(57) 6.1(43) 4.8	–
178	110(61) 270(39) 208	86(59) 220(41) 172	1.3(57) 4.4(43) 3.5	–
228	90(41) 220(59) 191	50(65) 153(35) 114	1.2(59) 4.1(41) 3.2	–
278	35(60) 66(40) 52	26(68) 121(32) 91	1.0(53) 3.1(47) 2.5	–
298	18(63) 38(34) 29	20(68) 104(32) 80	0.8(44) 2.3(56) 2.0	–

[a] $\chi^2 \geq 3$ (monoexponetial fit) and $\chi^2 \leq 1.5$ (biexponential fit) for all samples and temperatures (Figure S6). [b] Impossible to measure owing to the low phosphorescence intensity registered.

To summarize, a considerable increase in the phosphorescence emission was obtained by the incorporation of phenyl halides into the pores of the PCP, in comparison with incorporation of the nonaromatic halide derivative. This enhancement was a result of a structural transformation and is ascribed to the strong interaction between the phenyl halide and the dpNDI phosphor through CT complexation, which likely implies an extra population process of the triplet state (Scheme 1).

3. Conclusions

Phosphorescence emission at room temperature was turned on by the confinement of halogenated guests in the nanopores of the PCP, as a result of the high local halogen concentration close to the dpNDI phosphor. Such an environment induced an effective spin-orbit coupling, which increased the probability of radiative deactivation from the triplet state and reduced nonradiative deactivation pathways by avoiding self-quenching of the dpNDI phosphor. Moreover, with aryl halide guests the phosphorescence efficiency was considerably higher (around sixfold) than with nonaromatic guests; this phenomenon was a result of a structural transformation that allows a strong interaction through CT complexation with the dpNDI ligand in the framework, which also provides an extra population process of the triplet state. Also, the phosphorescence quantum yield increased by approximately one order of magnitude when the system was frozen at 77 K, because of the reduction of intramolecular motions (rotations and vibrations) and intermolecular collisions (mainly by molecular oxygen).

The long-lived photoinduced triplet states demonstrated in this material, together with the intrinsic gas-storage ability of MOFs, may open the door for further applications, for example, as efficient mesoscopic singlet oxygen generators. Moreover, the emission wavelength obtained in the red-visible/near-IR window could make these MOFs interesting for bio-imaging applications.

Experimental Section

The powder of $[Zn_2(bdc)_2(dpNDI)]_n$ (previously suspended in *N*,*N*-dimethylformamide) is filtered and soaked in the neat liquid of each guest to ensure that all the pores are filled. The stability of the PCP (absence of leaching of dpNDI) was checked by recording the absorption spectra of the supernatant after centrifugation of the powder. The size of the crystals was smaller than 200 nm to ensure stable suspensions.

TGA was carried out on the powder after drying the samples in vacuo at room temperature for 1 h to remove the guests attached to the outside of the crystals by using a Mettler Toledo Thermogravimetric Analyzer, model TGA/SDTA851e in the temperature range of 30–500 °C under flowing N_2 gas at a heating rate of 10 °C min^{-1}.

Steady-state emission spectra were recorded for the suspension obtained by dispersing the powder into the different guest solvents under continuous stirring in a SPEX spectrofluorimeter (model HORIBA Fluorolog-3), with 1 cm quartz cuvettes, at direct excitation of dpNDI[19,20] (380 nm). Phosphorescence spectra were measured after excitation at 380 nm in the same spectrofluorimeter with a flash lamp with a 50 μs delay after the flash and a gate time of 61 μs, accumulating 100 flash counts per point.

Absolute photoluminescence quantum yield was measured by using an integrating sphere system (Hamamatsu, C9920-02) at room temperature.

Phosphorescence decay curves were measured in a spectrofluorimeter (Edinburgh Instruments, model FL920) with a xenon flash lamp at 370 nm excitation and at the maximum of the phosphorescence emission accumulating 10000 counts at the maximum channel, repetition rate 10–100 Hz and time window from 0.4 to 80 ms depending on the sample (5–10 times higher than the estimated phosphorescence lifetime). The decays were analyzed by fast software 3.4.1 (Edinburgh Instruments).

The measurements were taken at different temperatures from 77 to 298 K controlled by Optista DN cryostat and ITC601 temperature controller (Oxford Instruments).

Acknowledgements

The authors gratefully acknowledge financial support from the Basque Government (IT339-10) and ERATO "Kitagawa Integrated Pores Project" of the Japan Science and Technology Agency. iCeMS is supported by the World Premier International Research Initiative (WPI), MEXT Japan. V.M.M. and R.S.Ll. acknowledge Ministerio de Economía y Competitividad for Ramón y Cajal (RYC-2011-09505) and Universidad del País Vasco (UPV-EHU) for research contract and predoctoral fellowship, respectively.

Keywords: halide aromatic guests · host–guest systems · luminescence · naphthalenediimide · porous coordination polymer

[1] R. C. Evans, P. Douglas, C. J. Winscom, *Coord. Chem. Rev.* **2006**, *250*, 2093 – 2126.
[2] O. Koshevoy, C.-L. Lin, A. J. Karttunen, M. Haukk, C.-W. Shih, P.-T. Chou, S. P. Tunik, T. A. Pakkanen, *Chem. Commun.* **2011**, *47*, 5533 – 5535.
[3] V. V. Grushin, N. Herron, D. D. LeCloux, W. J. Marshall, V. A. Petrov, Y. Wang, *Chem. Commun.* **2001**, 1494 – 1495.
[4] H. Guo, M. L. Muro-Small, S. Ji, J. Zhao, F. N. Castellano, *Inorg. Chem.* **2010**, *49*, 6802 – 6804.
[5] M. A. Baldo, M. E. Thompson, S. R. Forrest, *Pure Appl. Chem.* **1999**, *71*, 2095 – 2106.
[6] *Fluorescence and Phosphorescence* (Eds.: D. Rendell, D. Mowthorpe), Wiley, New York, **1987**.
[7] B. Valeur, *Molecular Fluorescence: Principles and Applications*, Wiley-VCH, Weinheim, **2001**.
[8] J. Kuijt, F. Ariese, U. A. Th. Brinkman, C. Gooijer, *Anal. Chim. Acta* **2003**, *488*, 135 – 171.
[9] R. J. Hurtubise, A. L. Thompson, S. E. Hubbard, *Anal. Lett.* **2005**, *38*, 1823 – 1845.
[10] O. Bolton, K. Lee, H.-J. Kim, K. Y. Lin, J. Kim, *Nat. Chem.* **2011**, *3*, 205 – 210.
[11] P. Montes-Navajas, L. Teruel, A. Corma, H. Garcia, *Chem. Eur. J.* **2008**, *14*, 1762 – 1768.
[12] A. Segura-Carretero, A. Salinas-Castillo, A. Fernández-Gutiérrez, *Crit. Rev. Anal. Chem.* **2005**, *35*, 3 – 14.
[13] D. S. McClure, *J. Chem. Phys.* **1949**, *17*, 905 – 913.
[14] S. P. McGlynn, R. Sunseri, N. Christodouleas, *J. Chem. Phys.* **1962**, *37*, 1818 – 1824.
[15] A. Segura-Carretero, C. Cruces-Blanco, B. Cañabate-Díaz, J. F. Fernández-Sánchez, A. Fernández-Gutiérrez, *Anal. Chim. Acta* **2000**, *417*, 19 – 30.

[16] V. Ramamurthy, J. V. Caspar, D. F. Eaton, E. W. Kuo, D. R. Corbin, *J. Am. Chem. Soc.* **1992**, *114*, 3882 – 3892.
[17] P. Ganesan, J. Baggerman, H. Zhang, E. J. Sudhölter, H. Zuilhof, *J. Phys. Chem. A* **2007**, *111*, 6151 – 6156.
[18] S. Green, M. A. Fox, *J. Phys. Chem.* **1995**, *99*, 14752 – 14757.
[19] Y. Takashima, V. Martínez-Martínez, S. Furukawa, M. Kondo, S. Shimomura, H. Uehara, M. Nakahama, K. Sugimoto, S. Kitagawa, *Nat. Commun.* **2011**, *2*, 168.
[20] V. Martínez-Martínez, S. Furukawa, Y. Takashima, I. López Arbeloa, S. Kitagawa, *J. Phys. Chem. C* **2012**, *116*, 26084 – 26090.
[21] G. P. Wiederrecht, W. A. Svec, M. R. Wasielewski, T. Galili, H. Levanon, *J. Am. Chem. Soc.* **2000**, *122*, 9715 – 9722.
[22] G. P. Wiederrecht, W. A. Svec, M. R. Wasielewski, *J. Am. Chem. Soc.* **1999**, *121*, 7726 – 7727.
[23] W. Z. Yuan, X. Y. Shen, H. Zhao, J. W. Y. Lam, L. Tang, P. Lu, C. Wang, Y. Liu, Z. Wang, Q. Zheng, J. Z. Sun, Y. Ma, B. Z. Tang, *J. Phys. Chem. C* **2010**, *114*, 6090 – 6099.